International Journal of Nanomedicine

Dovepress

open access to scientific and medical research

Open Access Full Text Article

ORIGINAL RESEARCH

ECM Mimicking Biodegradable Nanofibrous Scaffold Enriched with Curcumin/ZnO to Accelerate Diabetic Wound Healing via Multifunctional Bioactivity

Sachin Yadav[1,*], Dilip Kumar Arya[1,*], Prashant Pandey[1], Sneha Anand[1], Anurag Kumar Gautam[1], Shivendu Ranjan[2], Shubhini A Saraf[1], Vijayakumar Mahalingam Rajamanickam[1], Sanjay Singh[1], Kumarappan Chidambaram[3], Taha Alqahtani[3], Paruvathanahalli Siddalingam Rajinikanth[1,4]

[1]Department of Pharmaceutical Sciences, Babasaheb Bhimrao Ambedkar University, Lucknow, India; [2]School of Nano Science and Technology, Indian Institute of Technology Kharagpur, Kharagpur, West Bengal, India; [3]Department of Pharmacology and Toxicology, King Khalid University, Abha, Saudi Arabia; [4]Department of Pharmaceutical Technology, School of Pharmacy, Taylor's University Lakeside Campus, Kuala Lumpur Malaysia

*These authors contributed equally to this work

Correspondence: Paruvathanahalli Siddalingam Rajinikanth, Department of Pharmaceutical Sciences, Babasaheb Bhimrao Ambedkar University, Lucknow, 226025, India, Email psrajinikanth222@gmail.com

Introduction: Foot ulceration is one of the most severe and debilitating complications of diabetes, which leads to the cause of non-traumatic lower-extremity amputation in 15–24% of affected individuals. The healing of diabetic foot (DF) is a significant therapeutic problem due to complications from the multifactorial healing process. Electrospun nanofibrous scaffold loaded with various wound dressing materials has excellent wound healing properties due to its multifunctional action.

Purpose: This work aimed to develop and characterize chitosan (CS)-polyvinyl alcohol (PVA) blended electrospun multifunctional nanofiber loaded with curcumin (CUR) and zinc oxide (ZnO) to accelerate diabetic wound healing in STZ-induced diabetic rats.

Results: In-vitro characterization results revealed that nanofiber was fabricated successfully using the electrospinning technique. SEM results confirmed the smooth surface with web-like fiber nanostructure diameter ranging from 200 – 250 nm. An in-vitro release study confirmed the sustained release of CUR and ZnO for a prolonged time. In-vitro cell-line studies demonstrated significantly low cytotoxicity of nanofiber in HaCaT cells. Anti-bacterial studies demonstrated good anti-bacterial and anti-biofilm activities of nanofiber. In-vivo animal studies demonstrated an excellent wound-healing efficiency of the nanofibers in STZ–induced diabetic rats. Furthermore, the ELISA assay revealed that the optimized nanofiber membrane terminated the inflammatory phases successfully by downregulating the pro-inflammatory cytokines (TNF-α, MMP-2, and MMP-9) in wound healing. In-vitro and in-vivo studies conclude that the developed nanofiber loaded with bioactive material can promote diabetic wound healing efficiently via multifunction action such as the sustained release of bioactive molecules for a prolonged time of duration, proving anti-bacterial/anti-biofilm properties and acceleration of cell migration and proliferation process during the wound healing.

Discussion: CUR-ZnO electrospun nanofibers could be a promising drug delivery platform with the potential to be scaled up to treat diabetic foot ulcers effectively.

Keywords: electrospinning, curcumin, zinc oxide, chitosan, polyvinyl alcohol, diabetic wound healing

Introduction

Chronic non-healing foot ulcers are one of the most severe and disabling complications of diabetes, leading to non-traumatic lower-extremity amputation. Patients with diabetic foot ulcers face severe restrictions in daily life, like, social isolation, reduced mobility and economic burden for clinical treatment.[1] Diabetic wound healing is a challenge due to its pathophysiological complexity.[2]

Received: 31 August 2022
Accepted: 23 November 2022
Published: 30 December 2022

Graphical Abstract

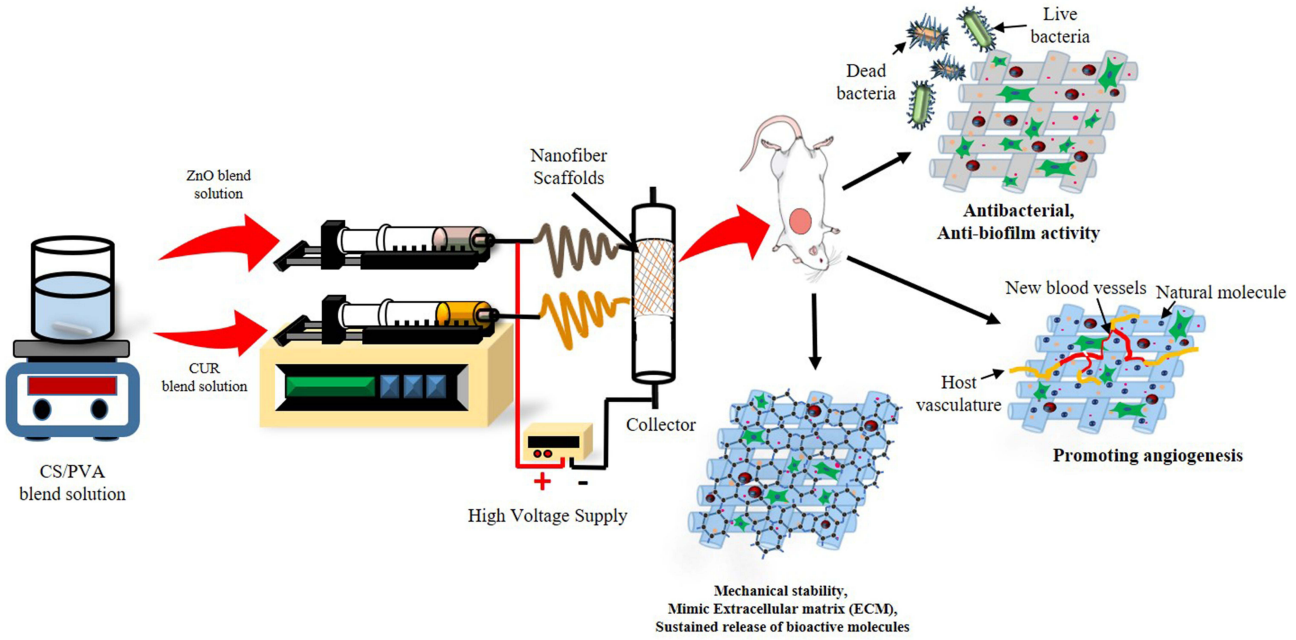

Various wound dressings have been using to treat diabetic ulcers as standard therapy; however, all these have been failed. Recently, biodegradable nanofibers have been considered as an ideal wound dressing and demonstrated tremendous potential for achieving rapid and complete healing of chronic diabetic wounds, delivering significantly improved results than conventional dressings.[3] The nanofiber has the same morphology as the natural extracellular matrix, a tunable shape and composition, and excellent drug loading. It possesses several unique wound healing properties, including a large surface area, absorbing wound exudates, providing a moisture environment, sustained and effective delivery of active substances, providing extracellular matrix (ECM) and preventing biofilm formation at the wound site.[4–7] In addition, they also promote cell migration, cell attachment, and proliferation, which are essential for cell growth and tissue regeneration.[5,8]

Chitosan (CS) is a linear polysaccharide derived from chitin, and PVA is a synthetic polymer. Both are biodegradable, biocompatible, non-toxic polymer, chosen to fabricate nanofibers. PVA is widely used for many biomedical applications, particularly in skin tissue regeneration and wound treatment,[9–11] and after combining with CS, it enhances the biodegradability, mechanical strength and hydrophilicity of hybrid nanofibers.[12,13] Additionally, it also improves the cell viability, proliferation and gene expression of fibroblast cells, hence promoting the electrospun membrane's cytocompatibility.[14,15]

Zinc is a vital micronutrient whose deficiency causes impaired cell regeneration and delayed wound healing.[16] Curcumin (CUR) is an emerging potent bioactive molecule having antioxidant, anti-inflammatory and anti-bacterial properties; however, its insolubility limits its clinical applications.[17,18] Several techniques have been used to fabricate nanofibers in which electrospinning is widely regarded as one of the most efficient, robust and cost-effective techniques.[19] Owing to the excellent wound healing properties of chitosan (CS), polyvinyl alcohol (PVA), good therapeutic properties of curcumin (CUR) and zinc oxide (ZnO), nanofiber scaffolds comprised of these molecules may be suitable for wound dressings.[20]

As per the literature mining, there is a need to formulate a DFU dressing material satisfying all mentioned criteria for ideal wound dressing. In this work, authors have attempted to formulate electrospun nanofibers with multifunctional capabilities as such (i) a sustained and controlled release of bioactive compound, (ii) better

absorption of wound exudates, (iii) potent antimicrobial, anti-biofilm properties and (iv) better cell migration and proliferation.

Materials and Methods

Materials

CS and PVA were purchased from HiMedia Laboratories Pvt. Ltd. (Mumbai, India). ZnO (Batch No. G05Z/2005/0807/08) was purchased from SD Fine-Chem Ltd. (Mumbai, India). All other chemicals and reagents were of analytical and HPLC grade.

Preparation of Polymer Blends

CS (2% w/v) in 1% acetic acid and PVA (10% w/v) in distilled water were dissolved and mixed in the ratio of 1:3. The CS/PVA mixture was split into two parts, and ZnO (1% w/v) was combined in one to make CS/PVA/ZnO, while CUR (5% w/v) was added to the other to make CS/PVA/CUR.

Fabrication of Nanofibers

The nanofibers were prepared by electrospinning techniques as described in our earlier work.[21] In brief, pre-prepared CS/PVA/CUR and CS/PVA/ZnO blends were loaded into 5 mL plastic syringe with a 21-gauge needle. Connected with power source at 20 kV, applied voltage and distance were maintained at 10 cm. Solutions were electrospun at a flow rate of 1 mL/h, and nanofibers were collected. The obtained nanofibers were cross-linked with glutaraldehyde (GA) vapour (50% v/v) for 1 hr in a desiccator containing glutaraldehyde solution. The cross-linked nanofiber formulations were stored at room temperature for 24 hrs in an oven, to remove excess of untreated GA.

Characterization

Nanofibers Morphology

The surface morphology and diameter of prepared nanofibers were measured using scanning electron microscopy (SEM) (FEI-SEM, Quanta 200). Images were captured at a voltage of 10 kV and later at some fixed magnifications. The average diameter of nanofibrous scaffolds at random locations was measured by ImageJ software.

FTIR Analysis

FTIR was used to confirm the structural and functional groups of CS, PVA CUR, ZnO and CS-PVA-ZnO-CUR electrospun nanofibers. FTIR peaks at frequencies scanning from 4000 to 400 cm^{-1} were used to confirm the functional group changes.

Mechanical Strength

The tensile strength of optimized nanofibers was measured using an ASTM tensile tester single-column (Zwick Roell Z010, Germany). The nanofiber scaffolds were cut into 10 cm, and their ends were coupled to the tensile tester's holding devices. All nanofibers were examined at 0.11 mm/s using a 5.0 kg load cell. The tensile strength of all the nanofibers was measured using the slopes of the stress–strain curves. The following formula was used to measure the ultimate tensile strength (UTS) and elongation at break (E_b).[3,22]

$$E_b = \frac{L_{max}}{L_o} \times 100$$

$$UTS = \frac{F_{max}}{A}$$

Where, L_{max} is moment of rupture on extension (m), L_0 is sample length, F_{max} is maximum load and A is sample's cross-sectional area.

Water Retention Capacity

The water absorption ability of CS-PVA-ZnO-CUR and CS-PVA-ZnO-CUR (CL) nanofibers was evaluated by incubating them at room temperature in PBS (pH 7.4). Briefly, the dry weight (W_d)of nanofibrous mat of 1 × 1 cm^2 size was determined and submerged in PBS (pH 7.4) for 24 hrs. At specified intervals samples were obtained from medium and residual water content on the surface was washed off. The wet weight (W_w) of the sample was determined instantly.[23] The following equation was used to determine the degree of water absorption.

$$Water\ retention(\%) = \frac{W_w - W_d}{W_d}$$

W_w is the sample's wet weight, and W_d is the sample's dry weight.

In-vitro Biodegradation

The degradation behaviour of nanofibers was investigated using weight loss at varying time intervals. The nanofiber scaffolds were vacuum-dried at 50 °C for 24 hrs, sliced into 1 × 1 cm^2 and weighed. The nanofibers were immersed in test tubes containing 10 mL PBS (pH 7.4) and 3 mg lysozyme (104 units/mL) in order to assess enzymatic degradation as well as to simulate the physiological body environment. The nanofibers were removed from the enzyme solution, washed with deionized water, dried for half an hour, and weighed every 24 hrs for 14 days to assess weight loss (W_L).[24]

$$W_L(\%) = \frac{W_i - W_t}{W_i} \times 100$$

Where $W_i$is the initial weight and W_t is the weight of nanofiber after time t.

In-vitro Drug Release

The in-vitro drug release from electrospun nanofibers was determined by incubating up to 72 hrs at 100 rpm in 10 mL fresh PBS at 37 °C (pH 7.4) with gentle shaking in a controlled shaker incubator. At pre-definite time intervals, 1 mL sample aliquots were withdrawn and replaced with 1 mL of freshly prepared PBS (pH 7.4) to maintain the sink condition. The amount of CUR and ZnO released from the nanofibrous scaffolds was determined spectrophotometrically at 424 nm and 361 nm, respectively.

Antimicrobial Activity

Zone of Inhibition Formation

The antimicrobial activity of nanofibers was determined using the disc diffusion method of agar well towards Gram-ve, *Pseudomonas aeruginosa* (ATCC 27853, Boston, MA, USA) and Gram+ve bacteria, *Staphylococcus aureus* (ATCC 25923, Seattle, WA, USA).[24] For 24 hrs, *P. aeruginosa* was cultured using Luria Bertani broth (LB) and *S. aureus* using Tryptone soy broth (TSB) (HiMedia LQ508) aqueous media in an orbital shaker at 37 °C and 200 rpm. The bacterial cultures were smeared in triplicate on MHA agar plate (Mueller Hinton) (HiMedia; M173). Six-millimeter wells were drilled using a sterile cork borer on the MHA plate under an aseptic environment. The drug-loaded nanofiber discs with diameter of 5 mm were pierced and kept under UV light sterilization for 2 hrs. A nanofiber disc, Gentamycin-soaked disc over *P. aeruginosa* and Vancomycin-soaked disc against *S. aureus* were applied as positive controls, while a placebo disc was left offsite in the agar well under aseptic condition. All the plates were incubated for 24 hrs at 37 °C. The anti-bacterial efficacy was determined and reported by measuring a clear inhibition zone in mm.[25]

Time-Kill Assay

A time-kill test was performed to assess the anti-bacterial activity in a specific time-dependent mode over *S. aureus* and *P. aeruginosa*.[3] In brief, nanofibrous scaffolds, a positive control (gentamycin 0.5 g/mL for *P. aeruginosa* and vancomycin 1 µg/mL for *S. aureus*) and a negative control were placed to a 1 mL culture of *P. aeruginosa* or *S. aureus* (as a starting inoculation, modified to 1 × 10^6 Cfu/mL). Antibiotics were supplied at a concentration that was less than half of the minimum inhibitory concentration. All test tubes were shaken at 150 rpm for 24 hrs at 37 °C in an orbital shaker. After plating the dilution factor (100 µL) on a Luria Bertani agar plate (for *P. aeruginosa*) and a Tryptic

soy agar plate (for *S. aureus*), the Cfu/mL concentrations were measured at 0, 8 and 24 hrs (for *S. aureus*). All plates were cultured at 37 °C for 24 hrs and CFU (colony forming units) counts were measured.

Microbial Penetration Test

Bacterial penetration of the wound is the initial stage in pathogenesis. Therefore, it would be fascinating to evaluate the nanofibrous scaffold's potential to prevent microbial invasion into the wound. Four glass vials were filled with nutrient broth (NB) medium; first, unwrapped and others wrapped with cotton plug, CS-PVA-ZnO-CUR and CS-PVA-ZnO-CUR (CL), respectively. The vials were kept at room temperature throughout the study. Bacterial growth in media-containing vials was determined after three and seven days. The vials plugged with cotton and vials left as open were taken as positive and negative control respectively. The ultraviolet spectroscopy (UV) at 600 nm and CFU were used to quantify microbial growth.[26]

Biofilm Assay

The biofilm assay was conducted as previously claimed with slight alterations.[27] *S. aureus* was cultured in glucose-free tryptic soy broth (TSB-0g) enriched with 1% NaCl and 0.5 gm/L glucose and *P. aeruginosa* was cultured in tryptic soy broth (HiMedia M011). Respective strains were grown in the appropriate media for 24 hrs before diluting 100X in fresh media and inoculating in triplicate in a 96-well microplate. The nanofibrous mats were punched 5 mm in diameter, UV sterilized for 2 hrs and incubated in triplicate wells with the control groups. For 24 hrs, the microtiter plates were then incubated at 37 °C with no shaking. The following days, nanofibrous scaffolds were scraped and discarded the culture. To fix the biofilm, non-adherent cells were cleaned three times with PBS pH (7.4) and each well received 150 µL of 95% ethanol for 2 minutes. Three times the wells were cleaned with 150 µL PBS pH (7.4) before being stained for 5 minutes with 150 µL of 1% w/v crystal violet (w/v). The wells were then cleaned three times with PBS pH (7.4) and air-dried. The biofilm intensity was analyzed using a plate reader at 570 nm.[24]

MTT Assay

In a 96-well, HaCaT cells (NCCS, Pune, India) were placed in 100 µL of DMEM media at a density of 1×10^4 cells per well and cultured for 24 hrs. After replacing the medium with nanofibers, the plates were incubated for 24 hrs. Afterwards, each well-received 10µL of MTT at a 5 mg/mL concentration in solution was kept for an additional 4 hrs. The purple colour formazan was dissolved by injecting 100 µL DMSO into all wells, kept at 37 °C for about 30 minutes. The absorbance at 570 nm was measured using a plate reader.[26,28]

Induction of Hyperglycaemia

Diabetes was induced in overnight starved rats using a single intraperitoneal injection of Streptozotocin (STZ), 60 mg/kg in freshly produced 0.1M citrate buffer (pH 4.00). For the preparation of STZ solution, 100 mg STZ was dissolved in 10 mL of 0.1 M citrate buffer pH 4. The blood glucose level was measured 72 hrs later using a standard glucometer (Bayer Contour TS Blood Glucose Monitor). As wound models, animals bearing a blood sugar level greater than 250 $mgdL^{-1}$ were used.[29]

In-vivo Studies

The wound-healing study was conducted in STZ-induced diabetic rats (Albino Wistar male rats). Babu Banarasi Das Northern Indian Institute of Technology (BBDNIIT, Lucknow) animal ethics committee granted permission to use animals (Approval No. BBDNIIT/IAEC/2021/09). The rats were placed in separate cages under monitored conditions (25 °C temperature, 55% relative humidity (RH) and a 12 hrs light/dark cycle) and each group contains 6 animals. Standard feeding and water were given to the animals, and all experiments involving animals followed the National Institutes of Health's Guide for the Care and Use of Laboratory Animals (NIH Publication No. 18–23, 1985).

Wound Closure Study

Animals were anesthetized intraperitoneally with a mixture of ketamine (100 mg/kg) and xylazine (5 mg/kg), and hair from the dorsal area was removed. Wounds were created using a sterilized biopsy punch (8-mm dia) in all four groups (normal, negative, CS-PVA-ZnO-CUR and CS-PVA-ZnO-CUR (CL) groups) of rats. The nanofibers were applied to

treatment groups for 14 days. Photographs of the wounded area were captured on 0, 4, 9, and 14 days to examine wounds' physical presence and closure. The wound contraction was expressed as a percentage reduction in the wound area and was calculated using the following formula:

$$Wound\ closure(\%)=\frac{Area\ of\ original\ wound-Wound\ area\ at\ nth\ day}{Area\ of\ original\ wound}$$

where n is the measurement day.[30]

H&E Staining

The collected tissue samples were subjected to histological examination and stained with haematoxylin and eosin (H&E) after embedding in paraffin and were examined under the light microscope.[24]

ELISA Assay

Detection of inflammatory factors TNF-α, MMP-2 and MMP-9 levels play an important role in diabetic wound healing. The collected tissue sample homogenate was prepared, and ELISA assay was performed as per the manufacturer's guidelines of TNF-α, MMP-2, and MMP-9 by ELISA kit.[31]

Statistical Analysis

GraphPad Prism version 8.0 was used to examine the data, and significant differences were evaluated at $P < 0.05$. A one-way ANOVA was performed, followed by a multiple comparison test to compare the differences between all groups.

Results and Discussion

Morphology

The nanofiber was successfully prepared using an electrospinning technique for diabetic wound healing and cross-linked with glutaraldehyde vapor to sustain the drug release for a prolonged duration. The formulation parameters, like concentration of polymer, voltage (kV), the distance between the tip and collector and the flow rate, were optimized and selected based on the earlier published literature.[3,24] SEM image confirmed the surface topography, diameter and uniformity of developed nanofibers. The average diameter of CS-PVA-ZnO-CUR nanofiber was found to be 274.16 ± 91.43 nm as depicted in Figure 1A and their corresponding histogram in Figure 1B, whereas the average diameter of CS-PVA-ZnO-CUR (CL) nanofiber was found 297.38 ± 69.86 nm, Figure 1C and their histogram Figure 1D. As demonstrated in the SEM image, the developed nanofiber produced fine, smooth, and interlinked all-around structured nanofibrous scaffolds with web-like porous construction, which is an optimal property of nanofibers for wound healing (Figure 1A and C).

FTIR

The FTIR spectra of CUR, ZnO, CS, PVA and CS-PVA-ZnO-CUR nanofiber are depicted in Figure 2A. The FTIR spectra of nanofiber revealed similar peaks of CS and PVA by shifting the carboxy (COOH) group to 1563.98 cm^{-1}. The stretching vibrations of hydroxyl (-OH) groups showed up as a broad and prominent peak at 3432.67 cm^{-1}. The hydroxyl group in was expected to have widened significantly, responsible for the formation of intermolecular hydrogen bonding. Furthermore, the formation of hydrogen bonds between the oxygen of PVA and the OH groups of CS enabled the carboxylate bond to shift to a higher wavenumber. The existence of N-H at 3200–3500 cm^{-1} reveals that CS and PVA have established a C-N bond. It also implies that there is no NH_2 in CS and that a C-N bond has formed. Thus, the FTIR spectra of nanofiber revealed that ZnO and CUR were successfully incorporated into CS-PVA-ZnO-CUR nanofibers.

Mechanical Strength

The tensile properties of nanofiber are important to withstand the maximum stress to heal and repair the tissue effectively and to release the bioactive molecules in a sustained and controlled manner for a prolonged time of duration at the site of infection. Tensile strength of CS-PVA-ZnO-CUR and CS-PVA-ZnO-CUR (CL) measured and was found to be 6.54 ± 0.47

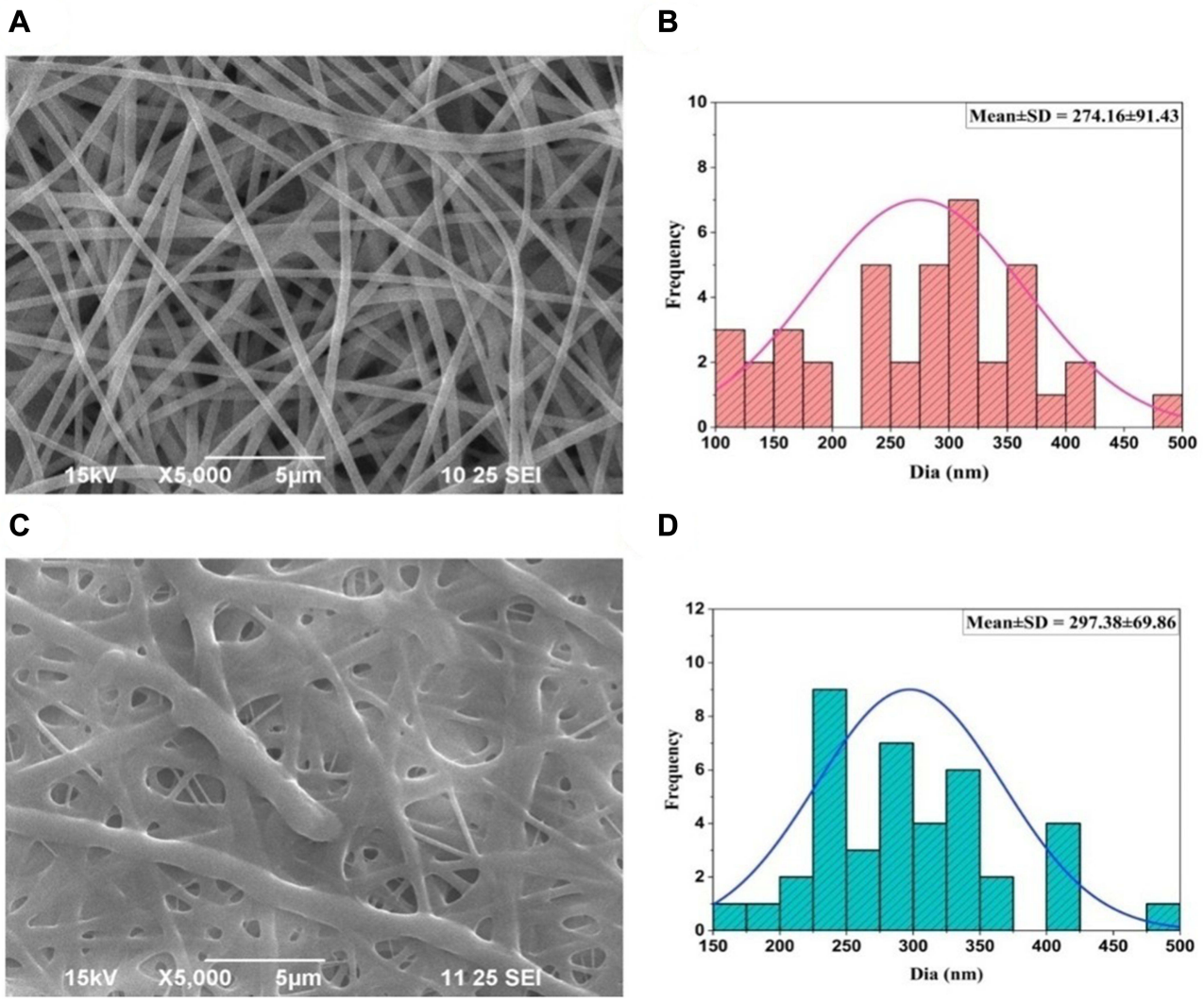

Figure 1 SEM photographs of nanofiber and their average diameter (**A**) CS-PVA-ZnO-CUR (**B**) average diameters (**C**) CS-PVA-ZnO-CUR (CL) and (**D**) average diameters.

and 10.21 ± 0.68 MPa, respectively (Figure 2B). It was observed that the cross-linking of nanofiber significantly improves the tensile strength of nanofiber.

Water Retention Capacity

The water absorption capacity and the amount of wound secretions that may be easily absorbed when placed on wounds were determined for CS-PVA-ZnO-CUR and CS-PVA-ZnO-CUR (CL) nanofiber for 24 hrs in PBS (pH7.4). The water retention capacity of CS-PVA-ZnO-CUR initially increases and reaches a maximum to 264.47% at 8hrs. After that, water retention capacity gradually decreased and after 24 hrs, it was 83.17%. On the other hand, the water retention capacity of CS-PVA-ZnO-CUR (CL) nanofiber was 134.72% after 8hrs and it started decreasing and it was 63.41% at the end of 24 hrs as shown in Figure 3A.

In-vitro Biodegradation

The rate of degradation of the CS-PVA-ZnO-CUR and CS-PVA-ZnO-CUR (CL) was determined by calculating scaffold weight loss by immersing in PBS (pH 7.4) and kept in mild shaking at 37 °C using lysozyme. The observed rate showed that CS-PVA-ZnO-CUR had degraded completely (99.67%) on day 10 in PBS at pH 7.4, whereas, after 14 days, the CS-

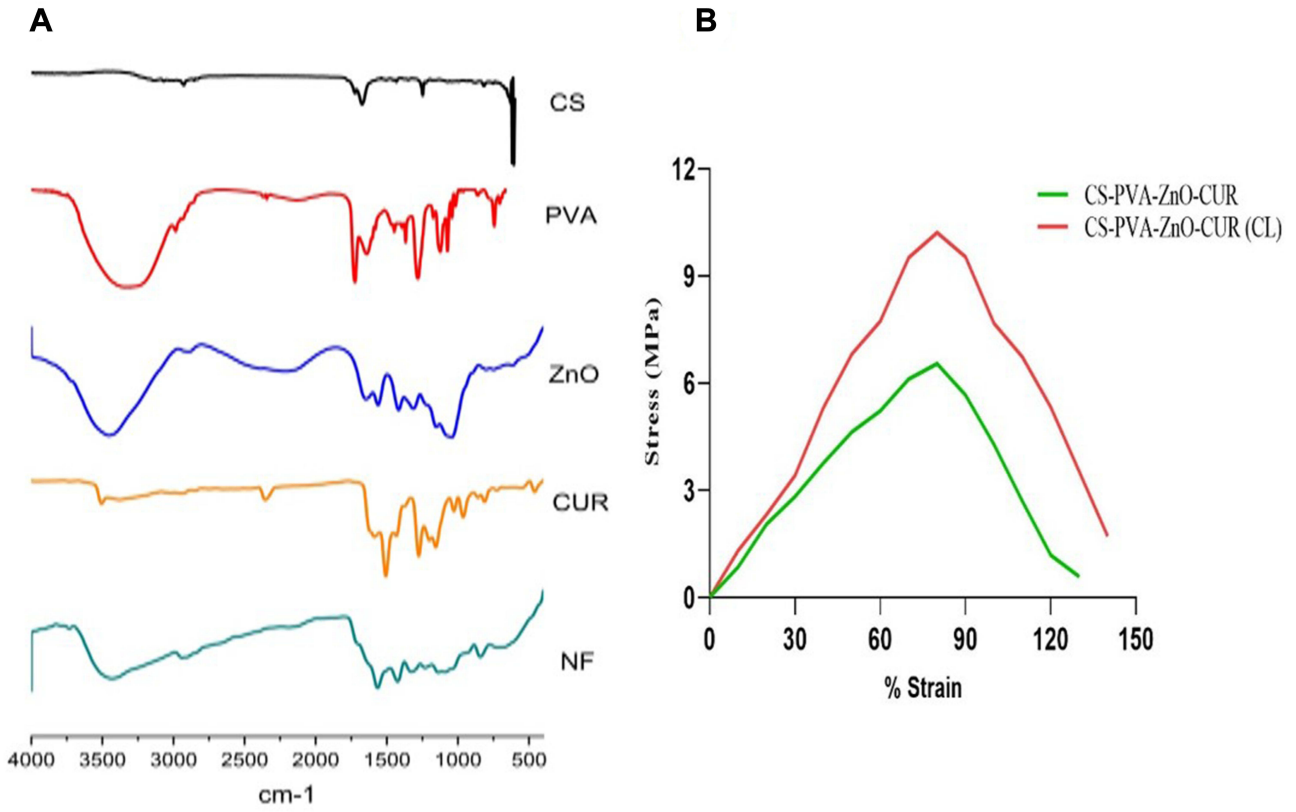

Figure 2 (**A**) FTIR spectra of CS, PVA, ZnO, CUR and CS-PVA-ZnO-CUR nanofiber and (**B**) tensile strength of CS-PVA-ZnO-CUR and CS-PVA-ZnO-CUR (CL) nanofiber.

PVA-ZnO-CUR (CL) had degraded by 92.13% (Figure 3B). The difference between the two formulations was due to both lipophilic characteristics; the greater the lipophilicity, the slower the formulation degrades.

In-vitro Drug Release

The optimized nanofiber formulation CS-PVA-ZnO-CUR and CS-PVA-ZnO-CUR(CL) was subjected to a CUR and ZnO release in PBS at pH 7.4 for 24 and 72 hrs, respectively, as shown in Figure 3C and D. The CUR and ZnO release from CS-PVA-ZnO-CUR showed release of 13.65% and 19.46% in the initial first one hour because of degradation of the polymer outer layer and release of drugs from the outer surface, followed by a slow pattern of release due to diffusion of the drugs from the inner core layer, whereas CUR and ZnO release from CS-PVA-ZnO-CUR(CL) nanofibers was found to be 3.89% and 7.32%, respectively, during the first 1 hr after that it followed more sustained and controlled drug release. This pattern of drug release demonstrates that the nanofibers developed can effectively carry medications to the wound site for a prolonged duration of time for efficient wound healing.

Antimicrobial Study

The developed nanofibers should maintain their potential to protect against microbial species as they are used in wound repair and tissue formation. The anti-bacterial effect of nanofiber by forming a zone of inhibition is shown in Figure 4A. The disc diffusion test results against *S. aureus* and *P. aeruginosa* revealed that the nanofiber exhibited a larger inhibition zone against both bacterial strains compared to control, as shown in Figure 4A-i) (F1, F2) and (A-ii) (F1, F2). The developed nanofibrous formulation has superior anti-bacterial properties against both bacteria. Furthermore, the inhibitory zone expands as the drug concentration in the nanofiber increases.[3] The bar diagram of the zone of inhibition produced by nanofiber formulations is shown in Figure 4B.

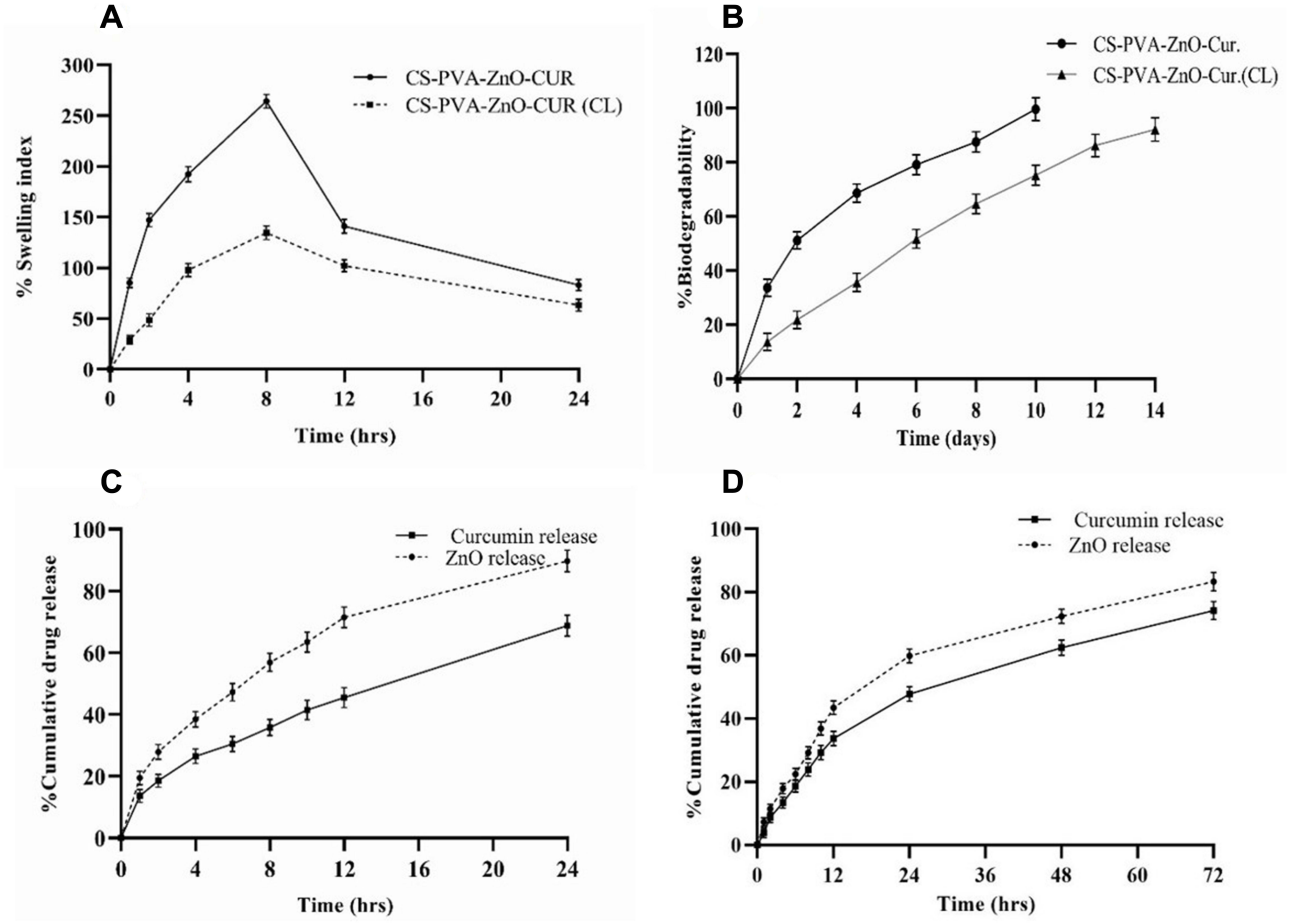

Figure 3 (**A**) Water retention capacity (**B**) in-vitro degradation study; in-vitro release of curcumin and zinc oxide (**C**) CS-PVA-ZnO-CUR and (**D**) CS-PVA-ZnO-CUR (CL) nanofibers in PBS pH (7.4).
Note: All the data is expressed as Mean±S.D (n = 3).

Time Kill Assay

The anti-bacterial activity of nanofiber formulation was time-dependent and determined by a time-kill assay against both *S. aureus* and *P. aeruginosa*. The results are indicated that CFU counts of both nanofiber formulations (CS-PVA-ZnO-CUR and CS-PVA-ZnO-CUR (CL)) decreased significantly as compared to the control *P. aeruginosa* and *S. aureus* cultures with drugs. Furthermore, it was noticed from Figure 4C and D that nanofiber formulations increased the anti-bacterial effect till 24 hrs due to the sustained release properties of nanofiber formulations.

Microbial Penetration

Adequate dressing and penetration barrier will prevent the wound from microbial invasion. This study used cotton-plugged vials as a positive control, indicating that the vial was devoid of microbiological contamination. However, an open vial employed as a negative control indicated turbidity after 3 and 7 days. According to Figure S1, only the negative control vial, which remained open, had turbidity and CFUs counts, indicating that the nanofiber-capped vial effectively protected against microbe invasion.

Biofilm Assay

Biofilm assay from Figure 5 indicated that *S. aureus* and *P. aeruginosa* had formed biofilm in the TSB-0 g enriched with 0.5% glucose and 1% NaCl and TSB media, respectively. The results (Figure 5A and C) clearly suggested that the newly developed CS-PVA-ZnO-CUR and CS-PVA-ZnO-CUR (CL) nanofibers restrict biofilm formation in both *S. aureus* and *P. aeruginosa*.

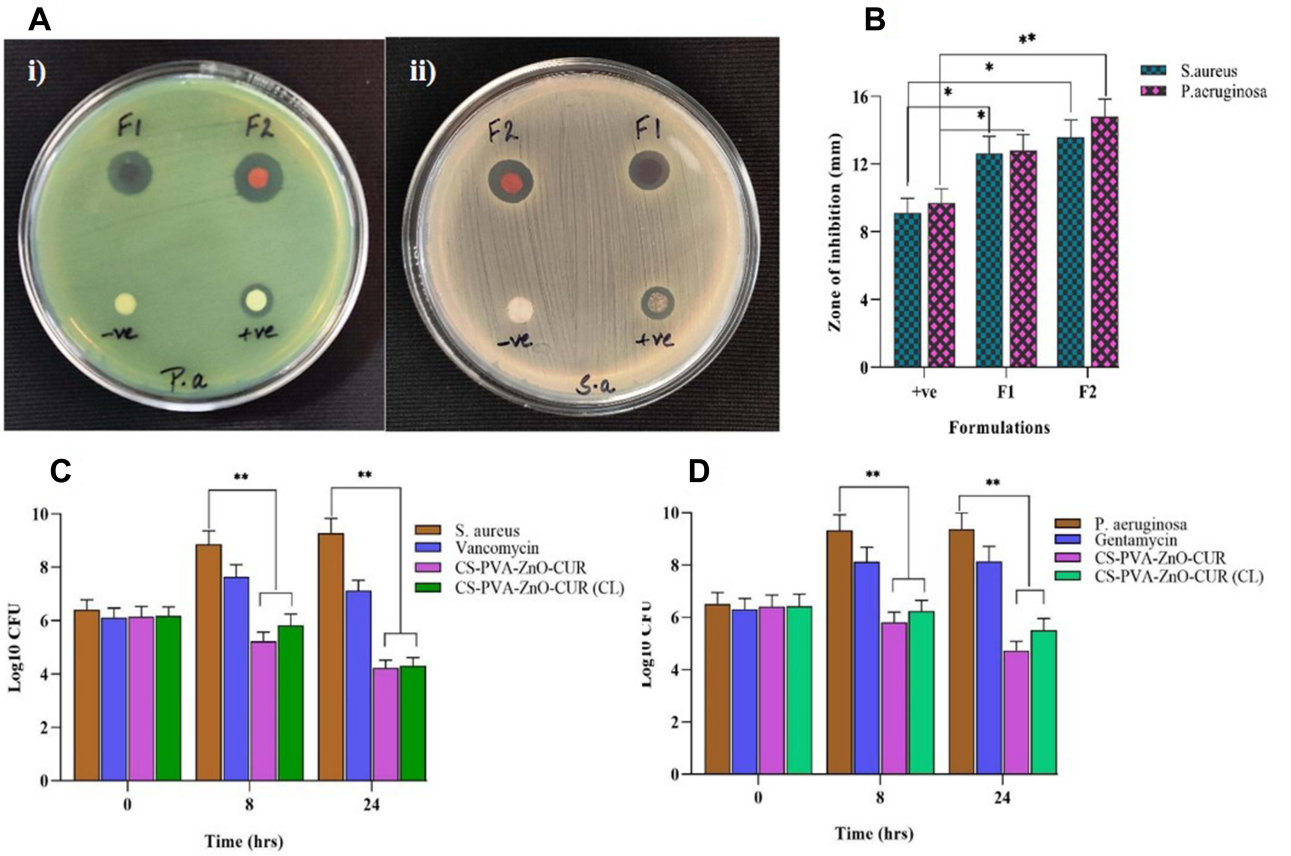

Figure 4 (**A**) Zones of the inhibition of nanofibers disc (F1: CS-PVA-ZnO-CUR (CL), F2: CS-PVA-ZnO-CUR, +ve control and -ve control) against *P. aeruginosa* and *S. aureus* and (**B**) bar diagram of disc diffusion test results; bar diagram of time-kill assay results against (**C**) *S. aureus* and (**D**) *P. aeruginosa*.
Note: *P < 0.05 and **P < 0.01 and data are shown as Mean±S.D.

MTT Analysis

The MTT was performed to ensure that the fabricated scaffolds were biocompatible. In-vitro cytotoxicity assays demonstrated reduced toxicity of CS-PVA-ZnO-CUR and CS-PVA-ZnO-CUR(CL) nanofibers scaffolds on HaCaT cells after 24 hrs of cultivation as compared to control, as illustrated in Figure 6A. As per the optical density (OD) of the MTT results, the number of cells grows continuously throughout 24 hrs, confirming that developed nanofibers were non-toxic on HaCaT cells.

In-vitro Scratch Assay

Keratinocytes migrate to heal the lesion and proliferate to build a dense epithelium during the reepithelization process (Figure 6C). Therefore, the in-vitro scratch assay of nanofibrous scaffolds was performed by observing fibroblast cell (HaCaT cells) ability to migrate in 0 and 48 hrs, respectively.

At 0 hr, the gap between scratched wounds was identical in all groups. CS-PVA-ZnO-CUR and CS-PVA-ZnO-CUR (CL) nanofibers enhanced significant cell migration after 48 hrs of incubation as compared to the control group Figure 6B. Despite the nanofibrous scaffold's excellent cell viability, biocompatibility and controlled degradation, it might induce sustained curcumin and ZnO delivery in the wounded area to fasten the re-epithelization process.

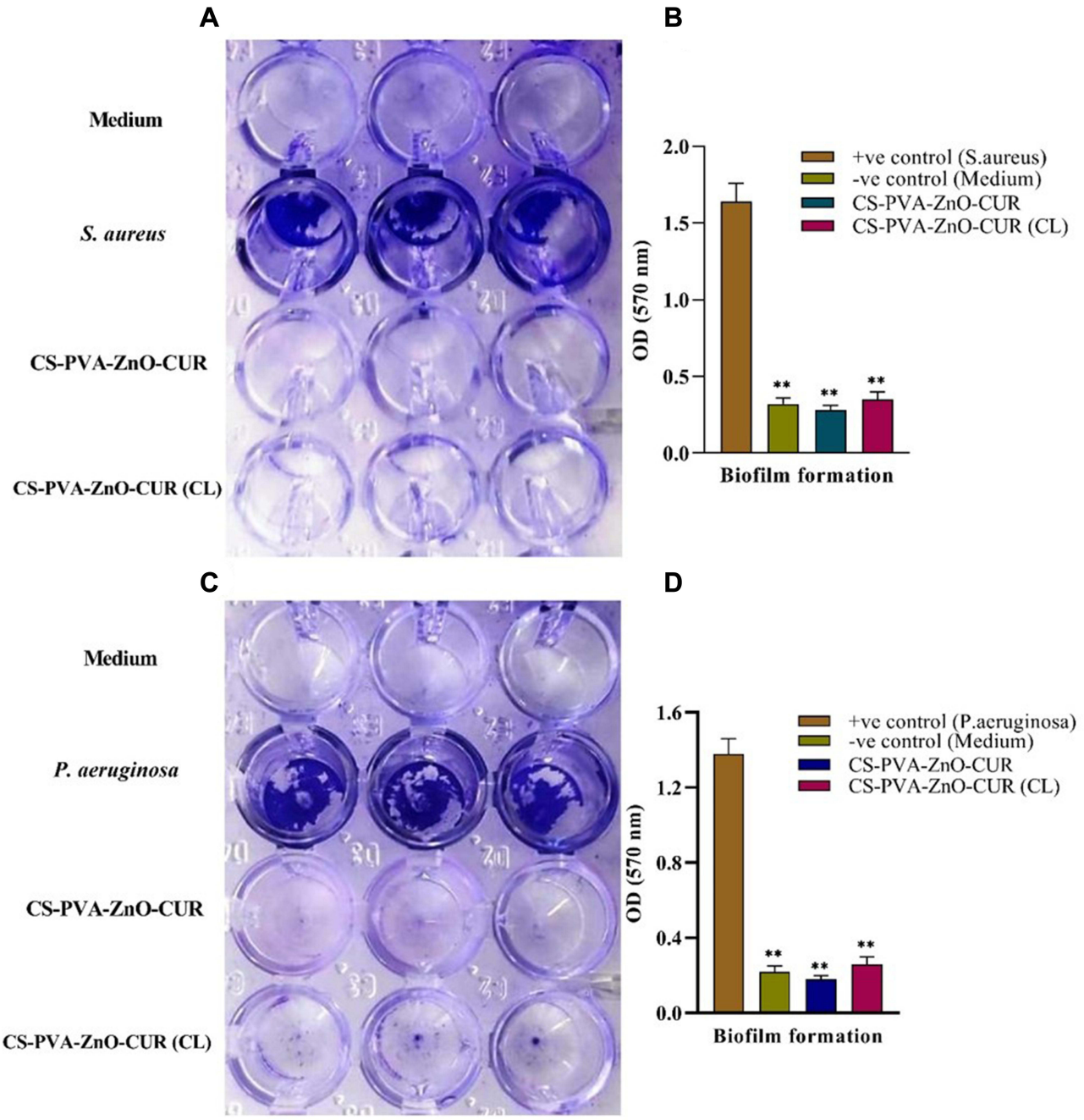

Figure 5 Biofilm formation in the presence of medium, bacteria, CS-PVA-ZnO-CUR and CS-PVA-ZnO-CUR (CL) nanofibrous mats.
Notes: (**A**) shows the microplate well before the absorbance reading and (**B**) represents the average absorbance of microplate well in triplicate for *S. aureus*, whereas (**C**) shows the microplate well before the absorbance reading and (**D**) represent the average absorbance of microplate well in triplicate for *P. aeruginosa*. **P < 0.01 which is considered as highly significant.

Hyperglycaemic Studies

All of the rats in this study showed symptoms of hyperglycaemia from the second day after administering STZ. Blood sugar levels increased considerably (P < 0.01) after 48 hrs of streptozotocin therapy and continued to rise throughout the trial as compared to the normal control group (Figure S2).

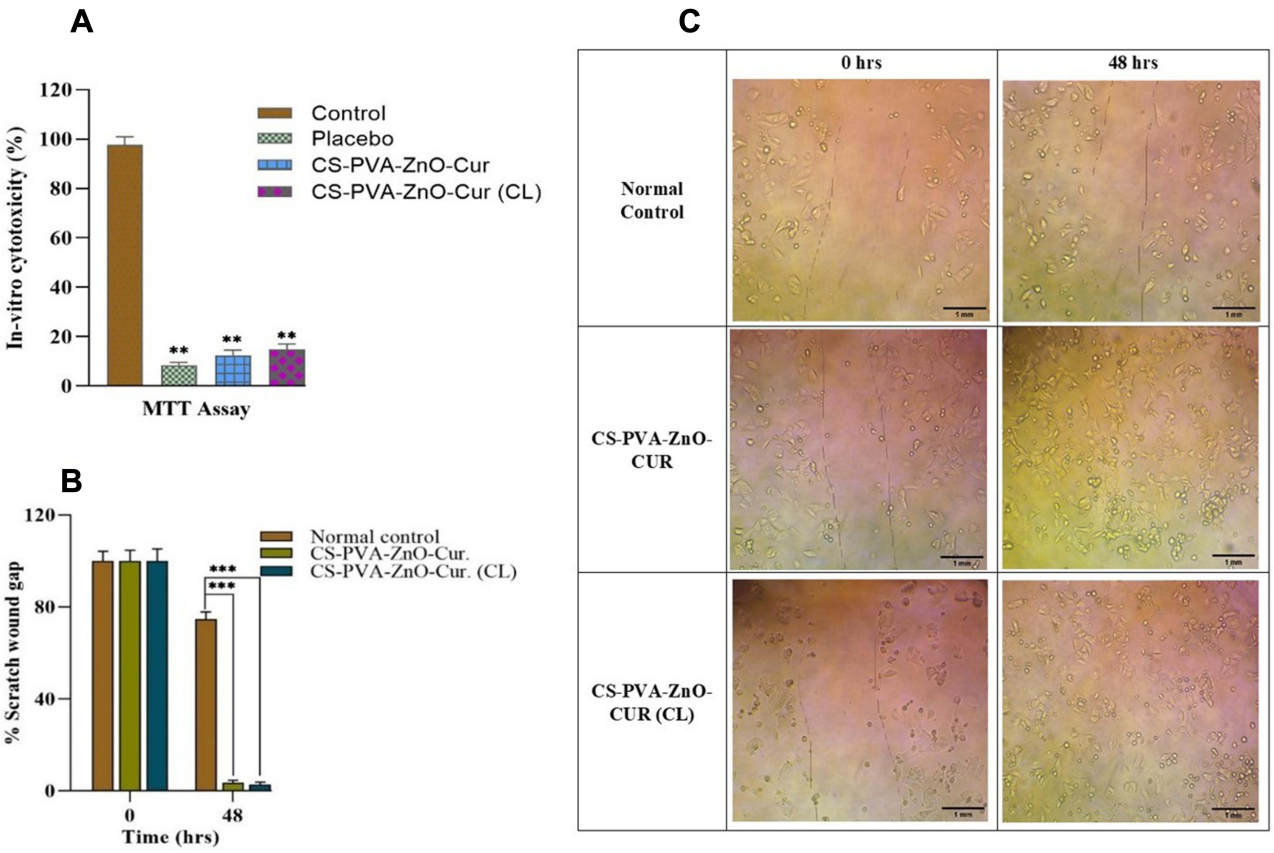

Figure 6 (**A**) In-vitro cytotoxicity of CS-PVA-ZnO-CUR and CS-PVA-ZnO-CUR (CL) by MTT test on HaCaT cells; (**B**) bar diagram of % scratch wound gap for in-vitro scratch assay at 0 and 48 hrs; (**C**) in-vitro scratch assay of control, CS-PVA-ZnO-CUR and CS-PVA-ZnO-CUR (CL) at 0 and 48 hrs.
Notes: Scale bar, 1 mm. **Differences between control and the formulations which are highly significant. $P < 0.05$ is considered significant and $P < 0.01$ is highly significant. ***$P < 0.001$ which is also considered as highly significant.

In-vivo Wound Healing Activity

The wound-healing ability of the developed nanofiber formulation was calculated by measuring wound closure in mm^2 for all the groups on days 0, 4, 9 and 14 as shown in Figure 7 using the ImageJ software at a 4 mm scale bar. The wound photograph images revealed clearly that the CS-PVA-ZnO-CUR and CS-PVA-ZnO-CUR (CL) nanofibrous formulations demonstrated a greater wound healing capacity than control groups on the 14^{th} day of treatment ($p < 0.01$) as shown in Figure S3.

The wound sizes of normal control, negative control, CS-PVA-ZnO-CUR, and CS-PVA-ZnO-CUR (CL) nanofibers were measured and found to be 50.094, 51.576, 50.351, and 50.004 mm^2, respectively, on day 0. On day 4^{th} the wound area for normal control and negative control were found to be 40.121 and 43.098 mm^2, respectively, which was higher than the wound area of CS-PVA-ZnO-CUR (31.67) and CS-PVA-ZnO-CUR (CL) (33.652) mm^2. Similarly, on day 9, the wound area of CS-PVA-ZnO-CUR (14.054 mm^2) and CS-PVA-ZnO-CUR (CL) (17.32 mm^2) was reduced significantly ($P < 0.01$) as compared to control groups (Figure 7). The minimum wound area was observed on day 14 for CS-PVA-ZnO-CUR and CS-PVA-ZnO-CUR (CL) groups as shown (Figure S2) and it was found to be 1.122 and 1.477mm^2, respectively, whereas the wound area of the normal and negative control groups was found to be 28.249 mm^2 and 23.682 mm^2, respectively, which was significantly higher as compared to nanofiber treated groups. Overall results from Figure 7, it was suggested that the developed nanofiber formulation exhibited excellent wound healing efficacy in the diabetic-induced animals due to nanofiber's multifunctional wound healing properties such as high surface volume ratio removing wound exudate, anti-bacterial effect, controlling of biofilm, sustained the delivery CUR and ZnO at the wound site, and promote tissue regeneration.

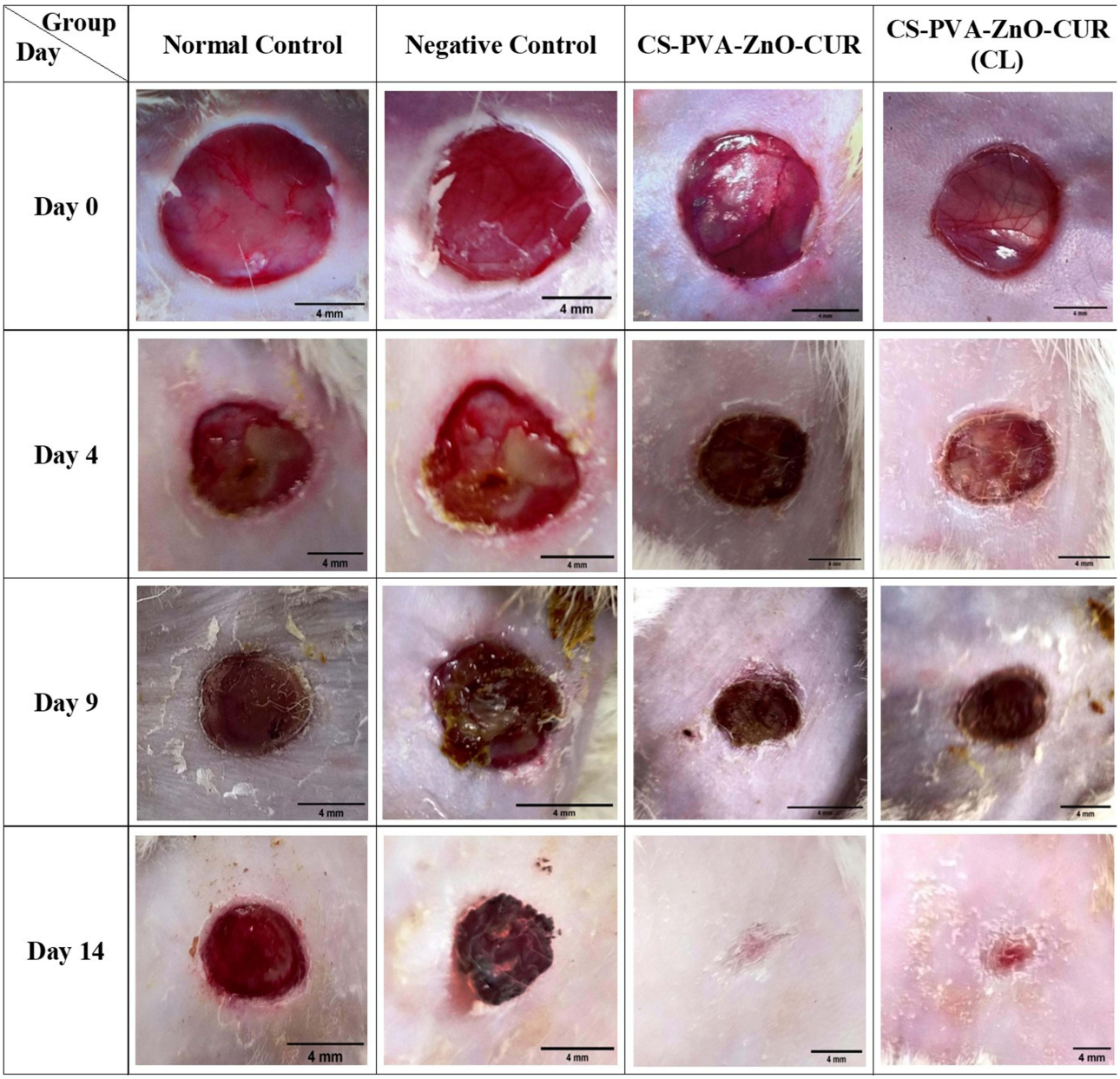

Figure 7 In-vivo images of the wound repairing process in diabetic rats on 0, 4th, 9th, and 14th day after treatment of rats with normal control, negative control, CS-PVA-ZnO-CUR and CS-PVA-ZnO-CUR (CL) (scale bar-4 mm).

Histopathological Studies

The histopathological improvements that occurred throughout the wound healing process were examined using haematoxylin and eosin staining of tissue samples from the treatment and control groups on days 4, 9, and 14 after creating the wound, and the findings are presented in Figure 8. Histological pictures taken on day 9 and 14 of wounded tissues treated with nanofiber revealed the presence of an intact keratin monolayer with homogenous epithelial cells. The skin cells were regenerated with more fibroblasts and less inflammatory cells, as depicted in Figure 9, indicating that the growth process had occurred as epithelial layer regeneration demonstrated. Moreover, fibrin and fibroblast were observed in substantial volumes in connective tissue, confirming collagen synthesis during wound healing. The absence of vascularization in groups treated with nanofiber supported the lack of any inflammatory cells. The nanofiber-treated groups completed wound regeneration and remodelling stages on day 14.

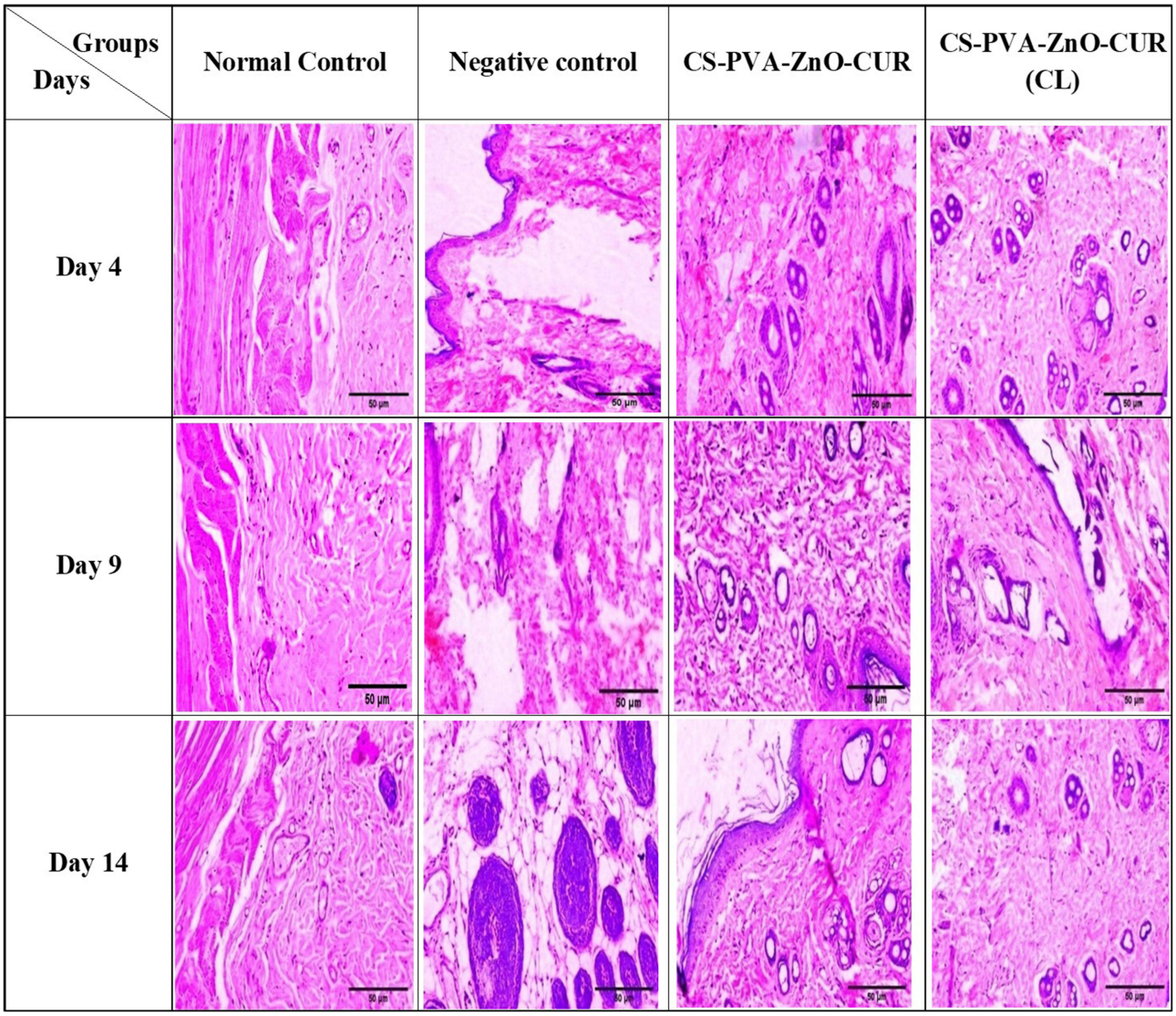

Figure 8 Histopathology images of normal control, negative control, CS-PVA-ZnO-CUR and CS-PVA-ZnO-CUR (CL) on day 4, 9 and 14.

ELISA Assay (TNF-α, MMP-2 and MMP-9)

Wound healing is linked by a complicated, inflammatory reaction involving several inflammatory cytokines, primarily interleukins, TNF-α, MMP-2 and MMP-9. TNF-α is the body's first and most crucial inflammatory mediator after trauma or infection. The increased level of TNF-α in diabetes promotes inflammation.[32] MMP-2 and MMP-9 play an essential role in wound healing by regulating angiogenesis, activating proangiogenic cytokines, cell signalling and promoting keratinocytes' migration during wound closure.[33,34] The levels of TNF-α, MMP-2 and MMP-9 were determined on days 0, 7 and 14-post treatment (Figure 9). On day 0, the level of TNF-α, MMP-2 and MMP-9 in normal control and treatment groups was not significantly different as compared to the toxic group, whereas on days 7 and 14 the level of TNF-α, MMP-2 and MMP-9 was significantly lowered in normal and treatment groups as compared to toxic control, indicating the proper wound healing in streptozotocin-induced diabetic rats.

Conclusion

Poor wound healing is amongst the most devastating consequences of diabetes, eventually leading to amputation. Electrospinning techniques were used to fabricate CS-PVA-ZnO-CUR nanofiber scaffolds successfully. SEM micro-photographs demonstrated that the prepared nanofiber showed a smooth, fine interconnected nanofiber with a web-like

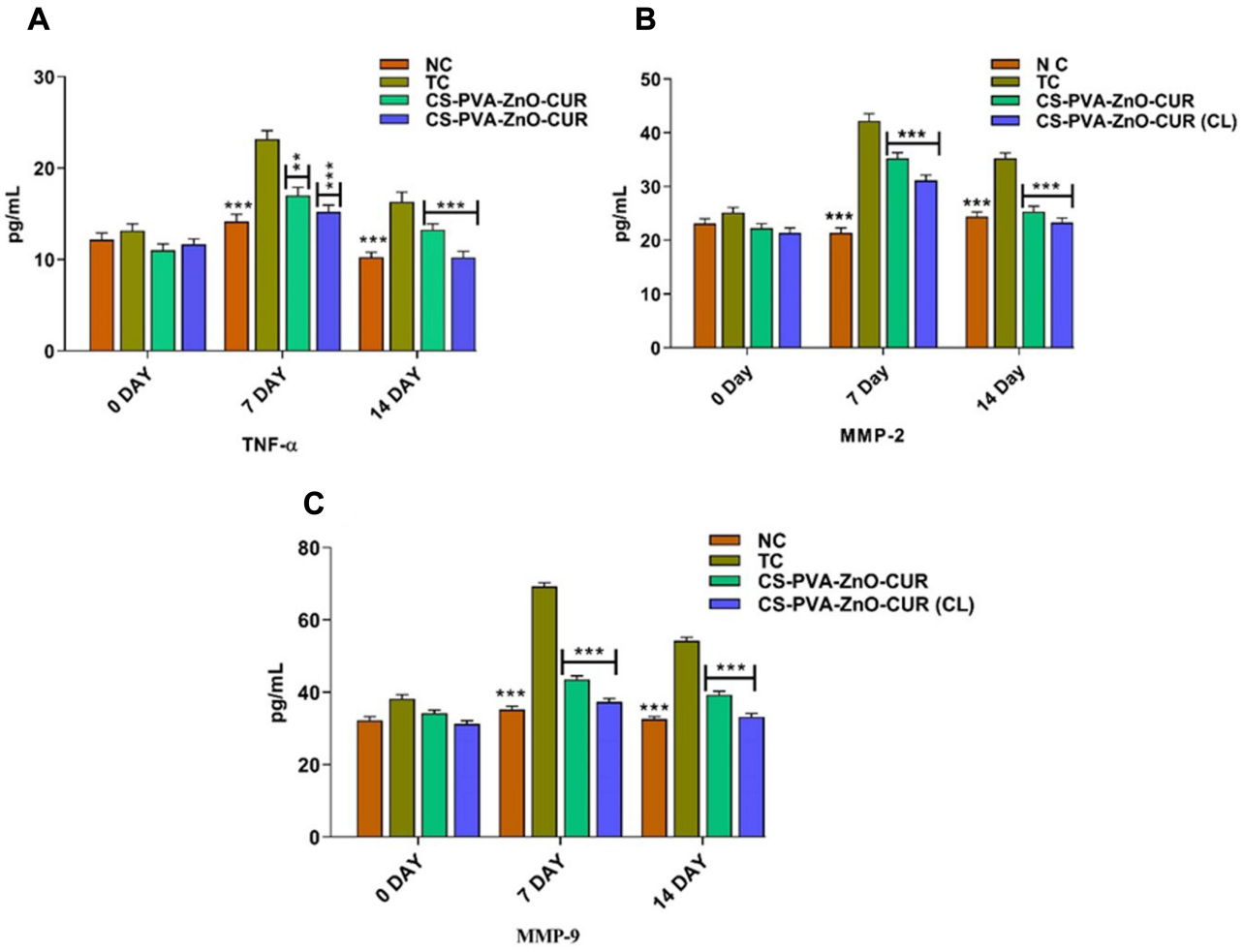

Figure 9 Concentrations of (**A**) TNF-α (**B**) MMP-2 and (**C**) MMP-9 at various stages of the wound repairing process.
Notes: The data is provided as Mean±S.D (n = 6). Statistically significant differences were found between the toxic control and test groups. The groups examined NC, TC, CS-PVA-ZnO-CUR, and CS-PVA-ZnO-CUR (CL). **P < 0.01 and ***P < 0.001 which is considered as highly significant.

structure, which are essential properties of nanofiber for wound healing. Optimized nanofiber batches possess sufficient mechanical strength, biodegradability and water retention capacity for better wound healing. In-vitro drug release studies confirmed nanofiber's sustained and controlled release characteristics for a prolonged period. Anti-bacterial studies demonstrated that fabricated nanofibers have excellent anti-bacterial potential efficacy and anti-biofilm ability of nanofiber against both *S. aureus* and *P. aeruginosa*.

Furthermore, the results demonstrated that ZnO, in addition to CUR, has synergistic antimicrobial effects. This would enable the fabricated scaffolds to serve as potential anti-bacterial wound dressings capable of preventing wound infection. The in-vitro cytotoxicity studies confirmed that our developed nanofibers are non-toxic on HaCaT cells. The cell migration assay findings in HaCaT cell lines demonstrate an increase in cell migration at the wound site to fill the gap, indicating that the developed nanofiber scaffolds' is having rapid wound-healing potential. The in-vivo studies in diabetically induced rats demonstrated clearly that CS-PVA-ZnO-CUR nanofiber significantly improved wound contraction ability during 14 days. Histology studies confirmed nanofiber's ability to re-epithelize and collagen formation during wound healing. According to the observations, the nanofiber formulation created has excellent attributes for diabetic wound healing in diabetic-induced rats and may be refined further for clinical studies. The higher scale-up ability of this formulation paved the way for future commercialization, suggesting that it may be effective for diabetic wound healing.

Data Sharing Statement

The authors confirm that the data supporting the findings of this study are available within the article and the raw data will be available on request to corresponding author.

Acknowledgment

The authors would like to acknowledge to DST-SERB (EEQ/2019/000429) for financial help for this work. The authors also would like to thank AICTE for providing GPAT scholarship for the research work. The authors extend their appreciation to the Deanship of Scientific Research at King Khalid University for supporting through Large Groups (RGP.2/52/1443). The authors would like to thank Prof. Shailendra Saraf, BBDNIIT for providing the animal facility and ethical approval for this project.

Disclosure

The authors report no conflicts of interest in this work.

References

1. Polikandrioti M, Vasilopoulos G, Koutelekos I., et al. Depression in diabetic foot ulcer: associated factors and the impact of perceived social support and anxiety on depression. *Int Wound J*. 2020;17(4):900–909. doi:10.1111/iwj.13348
2. Burgess JL, Wyant WA, Abdo Abujamra B, Kirsner RS, Jozic I. Diabetic wound-healing science. *Medicina*. 2021;57(10):1072. doi:10.3390/medicina57101072
3. Anand S, Rajinikanth PS, Arya DK, et al. Multifunctional biomimetic nanofibrous scaffold loaded with asiaticoside for rapid diabetic wound healing. *Pharmaceutics*. 2022;14(2):273. doi:10.3390/pharmaceutics14020273
4. Liu X, Xu H, Zhang M, Yu D-G. Electrospun medicated nanofibers for wound healing: review. *Membranes*. 2021;11(10):770. doi:10.3390/membranes11100770
5. Homaeigohar S, Boccaccini AR. Anti-bacterial biohybrid nanofibers for wound dressings. *Acta Biomaterialia*. 2020;107:25–49. doi:10.1016/j.actbio.2020.02.022
6. Abrigo M, McArthur SL, Kingshott P. Electrospun nanofibers as dressings for chronic wound care: advances, challenges, and future prospects. *Macromol Biosci*. 2014;14(6):772–792. doi:10.1002/mabi.201300561
7. Anjum S, Rahman F, Pandey P, et al. Electrospun Biomimetic Nanofibrous Scaffolds: a Promising Prospect for Bone Tissue Engineering and Regenerative Medicine. *Int J Mol Sci*. 2022;23(16):9206. doi:10.3390/ijms23169206
8. Zhu C, Cao R, Zhang Y, Chen R. Metallic ions encapsulated in electrospun nanofiber for antibacterial and angiogenesis function to promote wound repair. *Front Cell Dev Biol*. 2021;9:185.
9. Itoh H, Li Y, Chan KHK, Kotaki MJPB. Morphology and mechanical properties of PVA nanofibers spun by free surface electrospinning. *Polymer Bulletin*. 2016;73(10):2761–2777. doi:10.1007/s00289-016-1620-8
10. Wang M, Roy AK, Webster T. Development of chitosan/poly (vinyl alcohol) electrospun nanofibers for infection related wound healing. *Front Physiol*. 2017;7:683. doi:10.3389/fphys.2016.00683
11. Pandey P, Kumar Arya D, Kumar Ramar M, Chidambaram K, Rajinikanth PS. Engineered nanomaterials as an effective tool for HER2+ breast cancer therapy. *Drug Discov Today*. 2022;27(9):2526–2540. doi:10.1016/j.drudis.2022.06.007
12. Kouchak M, Ameri A, Naseri B, Boldaji SK. Chitosan and polyvinyl alcohol composite films containing nitrofurazone: preparation and evaluation. *Iran J Basic Med Sci*. 2014;17(1):14.
13. Fathollahipour S, Abouei Mehrizi A, Ghaee A, Koosha MJ. Electrospinning of PVA/chitosan nanocomposite nanofibers containing gelatin nanoparticles as a dual drug delivery system. *J Biomed Mater Res A*. 2015;103(12):3852–3862. doi:10.1002/jbm.a.35529
14. Sundaramurthi D, Vasanthan KS, Kuppan P, Krishnan UM, Sethuraman SJBM. Electrospun nanostructured chitosan–poly (vinyl alcohol) scaffolds: a biomimetic extracellular matrix as dermal substitute. *Biomed Mater*. 2012;7(4):045005. doi:10.1088/1748-6041/7/4/045005
15. Koosha M, Mirzadeh HJ. Electrospinning, mechanical properties, and cell behavior study of chitosan/PVA nanofibers. *J Biomed Mater Res A*. 2015;103(9):3081–3093. doi:10.1002/jbm.a.35443
16. Lin P-H, Sermersheim M, Li H, Lee PHU, Steinberg SM, Ma J. Zinc in Wound Healing Modulation. *Nutrients*. 2017;10(1):16. doi:10.3390/nu10010016
17. Karthikeyan A, Senthil N, Min T. Nanocurcumin: a Promising Candidate for Therapeutic Applications. *Front Pharmacol*. 2020;11:487. doi:10.3389/fphar.2020.00487
18. Urošević M, Nikolić L, Gajić I, Nikolić V, Dinić A, Miljković V. Curcumin: biological activities and modern pharmaceutical forms. *Antibiotics*. 2022;11(2):135. doi:10.3390/antibiotics11020135
19. Fadil F, Affandi NDN, Misnon MI, Bonnia NN, Harun AM, Alam MK. Review on electrospun nanofiber-applied products. *Polymers*. 2021;13(13):2087. doi:10.3390/polym13132087
20. Zhao R, Li X, Sun B, et al. Electrospun chitosan/sericin composite nanofibers with anti-bacterial property as potential wound dressings. *Int J Biol Macromol*. 2014;68:92–97. doi:10.1016/j.ijbiomac.2014.04.029
21. Agarwal Y, Rajinikanth PS, Ranjan S, et al. Curcumin loaded polycaprolactone-/polyvinyl alcohol-silk fibroin based electrospun nanofibrous mat for rapid healing of diabetic wound: an in-vitro and in-vivo studies. *Int J Biol Macromol*. 2021;176:376–386. doi:10.1016/j.ijbiomac.2021.02.025
22. Feng S, Zhang F, Ahmed S, Liu YJC. Physico-mechanical and anti-bacterial properties of PLA/TiO2 composite materials synthesized via electrospinning and solution casting processes. *Coatings*. 2019;9(8):525. doi:10.3390/coatings9080525

23. Waghmare VS, Wadke PR, Dyawanapelly S, Deshpande A, Jain R, Dandekar P. Starch based nanofibrous scaffolds for wound healing applications. *Bioact Mater*. 2017;3(3):255–266. doi:10.1016/j.bioactmat.2017.11.006
24. Anand S, Pandey P, Begum MY, et al. Electrospun Biomimetic Multifunctional Nanofibers Loaded with Ferulic Acid for Enhanced Antimicrobial and Wound-Healing Activities in STZ-Induced Diabetic Rats. *Pharmaceuticals*. 2022;15(3):302. doi:10.3390/ph15030302
25. Gong P, Li H, He X, et al. Preparation and anti-bacterial activity of Fe3O4@ Ag nanoparticles. *Nanotechnology*. 2007;18(28):285604. doi:10.1088/0957-4484/18/28/285604
26. Wsoo MA, Abd Razak SI, Bohari SPM, et al. Vitamin D3-loaded electrospun cellulose acetate/polycaprolactone nanofibers: characterization, in-vitro drug release and cytotoxicity studies. *Int J Biol Macromol*. 2021;181:82–98. doi:10.1016/j.ijbiomac.2021.03.108
27. Avila-Novoa M-G, Iñíguez-Moreno M, Solís-Velázquez O-A, González-Gomez J-P, Guerrero-Medina P-J, Gutiérrez-Lomelí MJ. Biofilm formation by Staphylococcus aureus isolated from food contact surfaces in the dairy industry of Jalisco, Mexico. *J Food Qual*. 2018;2018. doi:10.1155/2018/1746139
28. Muniandy K, Gothai S, Tan WS, et al. In Vitro Wound Healing Potential of Stem Extract of Alternanthera sessilis. *Evid Based Complementary Alternative Med*. 2018;2018:1–13. doi:10.1155/2018/3142073
29. Bulbake U, Jain S, Kumar N, Mittal A. Curcumin loaded biomimetic composite graft for faster regeneration of skin in diabetic wounds. *J Drug Deliv Sci Technol*. 2018;47:12–21. doi:10.1016/j.jddst.2018.06.016
30. Chen H, Peng Y, Wu S, Tan LPJM. Electrospun 3D fibrous scaffolds for chronic wound repair. *Materials*. 2016;9(4):272. doi:10.3390/ma9040272
31. Siqueira MF, Li J, Chehab L, et al. Impaired wound healing in mouse models of diabetes is mediated by TNF-alpha dysregulation and associated with enhanced activation of forkhead box O1 (FOXO1). *Diabetologia*. 2010;53(2):378–388. doi:10.1007/s00125-009-1529-y
32. Qiu H, Zhu S, Pang L, et al. ICG-loaded photodynamic chitosan/polyvinyl alcohol composite nanofibers: anti-resistant bacterial effect and improved healing of infected wounds. *Int J Pharm*. 2020;588:119797. doi:10.1016/j.ijpharm.2020.119797
33. Xu F, Zhang C, Graves DT. Abnormal cell responses and role of TNF-α in impaired diabetic wound healing. *Biomed Res Int*. 2013;2013:754802. doi:10.1155/2013/754802
34. Caley MP, Martins VLC, O'Toole EA. Metalloproteinases and Wound Healing. *Adv Wound Care*. 2015;4(4):225–234. doi:10.1089/wound.2014.0581